

Plant-Mediated Green Synthesis of Zinc Oxide Nanoparticles and their Biological Applications

Sagar D. Bhakare^{1*}, Vijay T. Godse¹, Sudhir B. Kumbhar¹, Dilip D. Anuse¹, Santosh B. Gaikwad²

Department of Chemistry, Dahiwadi College, Dahiwadi, Man, Dist. Satara, Maharashtra, India¹

Department of Chemistry, Late Pundalikrao Gawali Arts and Science Mahavidyalaya, Shirpur (Jain), Washim, Maharashtra, India²

sagarbhakare27@gmail.com^{1*}, vijaygodse100@gmail.com¹,

sudhirkumbhar15@gmail.com¹, dilipanuse11@gmail.com¹, sbgaikwad33@gmail.com²

*Corresponding Author: sagarbhakare27@gmail.com

Abstract: Nanotechnology offers vast potential in medicine, catalysis, and environmental applications. In this study, zinc oxide nanoparticles (ZnO NPs) were synthesized via an eco-friendly green method using *Dolichandrone falcata* leaf extract as a natural reducing and stabilizing agent. Phytochemical analysis confirmed the presence of flavonoids, phenolics, steroids, triterpenoids, and saponins, which facilitate nanoparticle formation and stabilization. The synthesized ZnO NPs were characterized by UV-Visible spectroscopy, FTIR, XRD, SEM, TEM, EDAX, DLS, and zeta potential analysis, confirming the formation of stable, crystalline nanoparticles with an average size of ~30 nm. Biological studies revealed significant antibacterial, antifungal, antioxidant, and anti-inflammatory activities, highlighting their biomedical potential. This study establishes plant-mediated ZnO nanoparticle synthesis as a sustainable and cost-effective approach for developing multifunctional nanomaterials with promising applications in healthcare, catalysis, and environmental science..

Keywords: Zinc oxide nanoparticles (ZnO NPs), *Dolichandrone falcata*, Phytochemicals, Nanotechnology, Anticancer activity, Antibacterial activity, Antioxidant activity, Nanocatalyst, Thiophene thiazole derivatives

I. INTRODUCTION

Nanotechnology, defined as the manipulation of matter at the nanoscale (1–100 nm), has significantly advanced diverse fields such as materials science, medicine, environmental remediation, and catalysis [1]. Nanoparticles (NPs) exhibit unique physicochemical properties, including high surface area-to-volume ratio, quantum confinement effects, and enhanced reactivity compared to bulk materials [2]. Among various nanomaterials, metal oxide nanoparticles (MONPs) have gained considerable attention due to their stability, tunable bandgap, and multifunctional applications [3]. Zinc oxide nanoparticles (ZnO NPs), in particular, possess a wide bandgap (3.37 eV) and high exciton binding energy (60 meV), enabling applications in optoelectronics, photocatalysis, and biomedicine [4]. Other MONPs such as TiO₂, CuO, Fe₂O₃/Fe₃O₄, and MgO exhibit distinctive properties including photocatalytic activity, antimicrobial potential, magnetic behavior, and thermal stability, respectively, supporting their wide-ranging industrial and biomedical applications [5–8]. Despite these advantages, challenges such as particle aggregation, toxicity at higher concentrations, and environmental persistence necessitate the development of controlled and sustainable synthesis strategies [9,10].

Nanoparticle synthesis methods are broadly categorized into top-down and bottom-up approaches [11]. Top-down methods, including mechanical milling, laser ablation, and sputtering, involve the breakdown of bulk materials into nanoscale particles but are often energy-intensive and may introduce impurities [12]. In contrast, bottom-up approaches such as sol-gel, co-precipitation, hydrothermal, and solvothermal methods enable controlled growth of nanoparticles from atomic or molecular precursors, offering improved uniformity and scalability [13–16]. However, conventional chemical synthesis routes frequently involve toxic solvents, surfactants, and reducing agents, posing environmental and



health concerns [17,18]. To address these limitations, green synthesis approaches utilizing biological systems—particularly plant extracts—have emerged as sustainable alternatives [19]. These methods employ natural phytochemicals as reducing and stabilizing agents, resulting in eco-friendly, cost-effective, and biocompatible nanoparticles. Green synthesis has been successfully applied for producing ZnO, TiO₂, and CuO nanoparticles with comparable or enhanced properties relative to chemically synthesized counterparts [20].

Plant-mediated synthesis of MONPs provides promising solutions to global challenges such as antimicrobial resistance, cancer, and environmental pollution [21,22]. ZnO NPs exhibit significant biological activities primarily through the generation of reactive oxygen species (ROS), membrane disruption, and biomolecular interactions [23]. They demonstrate notable anticancer activity by inducing apoptosis in cancer cell lines such as A549, while exhibiting comparatively low toxicity toward normal cells [24,25]. Additionally, ZnO NPs show strong antibacterial activity against pathogens such as *Xanthomonas* spp. and *Streptococcus pneumoniae* [26], as well as antifungal effects against *Alternaria* spp. and *Aspergillus niger* [27]. Their antioxidant properties involve scavenging of free radicals, while anti-inflammatory effects are mediated through cytokine suppression and enzyme inhibition [28,29]. Beyond biomedical applications, ZnO NPs function as efficient heterogeneous catalysts due to their Lewis acidity and high surface area [30,31]. These attributes align with sustainable development goals and green chemistry principles [32,33].

Dolichandrone falcata (family Bignoniaceae), commonly known as Medshingi or Wagati, is a medicinal plant widely distributed in arid regions of India and South Asia [34]. It is rich in bioactive phytochemicals such as flavonoids, alkaloids, tannins, saponins, glycosides, and phenolics, which contribute to its diverse pharmacological properties [35]. The plant has been traditionally used for its anti-inflammatory, antioxidant, anti-allergic, anxiolytic, and antimicrobial activities [36]. The presence of these phytoconstituents makes *D. falcata* leaf extract an effective bioreducing and stabilizing agent for nanoparticle synthesis, facilitating the formation of stable and functional nanomaterials.

In this context, the present study focuses on the green synthesis of ZnO nanoparticles using *D. falcata* leaf extract. The synthesized nanoparticles were systematically characterized using various analytical techniques, and their biological activities including antibacterial, antifungal, antioxidant, and anti-inflammatory effects were evaluated.

This work highlights a sustainable and interdisciplinary approach toward the development of multifunctional ZnO nanomaterials with potential applications in healthcare, catalysis, and environmental science.

II. MATERIAL AND METHODS

2.1. Preparation of Plant Extract

Fresh leaves of *Dolichandrone falcata* were procured from the hilly region of the Western Ghats in Maharashtra. The leaves underwent a dual washing process with deionized water, followed by shade drying for a duration of eight days, and were subsequently ground into a fine powder. A sample of this powder (10 g) was combined with 100 ml of deionized water and subjected to heating at 80°C with continuous stirring for 30 minutes. The resultant mixture was allowed to cool to room temperature and was then filtered using Whatman filter paper no. 41. The filtrate was stored at 4°C for future use.

2.2. Bio Synthesis of ZnO Nanoparticles

The synthesis of copper oxide nanoparticles was conducted using a 0.1 M solution of Zinc acetate as the precursor. A volume of 100 ml of this solution was placed in a 250 ml conical flask and subjected to stirring using a hot plate magnetic stirrer. Subsequently, 20 ml of plant extract was added dropwise to the solution with continuous stirring at 60°C for one hour. Following this, 2 M NaOH was introduced dropwise, adjusting the pH to 10, which resulted in the formation of a white precipitate. The solution was further stirred for an additional hour and then centrifuged at 5000 rpm. The resulting pellets were washed with deionized water and ethanol. The solid was dried at 100°C for 2 hours. The resulting yellowish white powder of ZnO nanoparticles was utilized for characterization.



2.3. Characterisation of biogenic Df-ZnO nanoparticles:

Biosynthesized ZnO NPs were analyzed using a UV-visible spectrophotometer (Bio Era BI/CI/SP/SDB-S-04) within the range of 200 – 600 nm. The crystalline nature was evaluated by X-ray diffraction technique using a Bruker D8 Venture instrument. The morphology of ZnO NPs was examined by scanning electron microscopy (JEOL JSM-IT200) and transmission electron microscopy by (JEOL - 2200FS). Elemental mapping was conducted using Energy dispersive X-ray spectroscopy (EDS). The association of ZnO NPs with phytochemicals was analyzed utilizing Fourier-transform infrared spectroscopy (LAMBDA-FTIR-7600). Particle size and zeta potential analysis was carried out by Malvern Nano ZS 90 ZEN 3696. Surface composition and oxidation state was analyzed by X-ray Photoelectron Spectroscopy (JEOL Japan, JPS-9030).

2.4. Antibacterial activity by well diffusion method-

The inoculum of the microorganism was prepared from the bacterial cultures. 15ml of nutrient agar (Hi media) medium was poured in clean sterilized Petri plates and allowed to cool and solidify. 100 µl of broth of bacterial strain was pipette out and spread over the medium evenly with a spreading rod till it dried properly. Wells of 6mm in diameter were bored using a sterile cork borer. Solutions of the compounds (100µl/ml) were prepared in DMSO and 100µl of prepared test solutions (1mg/ml) and standard was added to the wells. The petri plates incubated at 37°C for 24 h. Streptomycin (1mg/ml) was prepared as a positive control and DMSO was taken as negative control. Antibacterial activity was evaluated by measuring the diameters of the zone of inhibitions (ZI) all the determination were performed in triplicates.

2.5. Antifungal activity by well diffusion method:

The inoculum of the microorganism was prepared from the fungal cultures. 15ml of Sabouraud agar (Hi media) medium was poured in clean sterilized Petri plates and allowed to cool and solidify. 100 µl of broth of fungal strain was pipette out and spread over the medium evenly with a spreading rod till it dried properly. Wells of 6mm in diameter were bored using a sterile cork borer. Solutions of the compounds (100µl/ml) were prepared in DMSO and 100µl of prepared test solutions and standard was added to the wells. The petri plates incubated at 37°C for 24 h. Miconazole (1mg/ml) was prepared as a positive control and DMSO was taken as negative control. Antifungal activity was evaluated by measuring the diameters of the zone of inhibitions (ZI) all the determination were performed in triplicates.

2.6. In vitro Anti-Inflammatory by Protein Denaturation Assay:

The reaction mixture (10 mL) consisted of 0.4 mL of egg albumin (from fresh hen's egg), 5.6 mL of phosphate buffered saline (PBS, pH 6.4) and 100 µL of different concentration sample. Similar volume of double-distilled water served as control. Then the mixtures were incubated at (37°C ±2) in a incubator for 15 min and then heated at 70°C for 5 min. After cooling, their absorbance was measured at 660 nm by using vehicle as blank. Diclofenac sodium at the concentration was used as reference drug and treated similarly for determination of absorbance. The percentage inhibition of protein denaturation was calculated by using the following formula,

$$\% \text{ Inhibition} = C - T / C$$

Where,

T = absorbance of test sample

C = absorbance of control

2.7. Antioxidant Assay by DPPH Method:

Antioxidant activity of test material was estimated for their free radical scavenging activity by using DPPH (1, 1-Diphenyl-2, Picryl-Hydrazyl) free radicals. 1ml of different concentrations (20, 40, 60, 80, 100µg/ml) were taken in a test tubes. 1.5ml of 0.1% methanolic DPPH was added over the samples and incubated for 30 minutes in dark condition. The samples were then observed for discoloration; from purple to yellow and read the absorbance on colorimeter at 510 nm Radical scavenging activity was calculated by the following equation:



DPPH radical scavenging activity (%) = [(Absorbance of control - Absorbance of test sample) / (Absorbance of control)] x 100.

III. RESULT AND DISCUSSION

3.1. Phytochemical Screening:

Based on previously reported studies, the leaf extract contains flavonoids, phenolics, alkaloids, and glycosides, which act as reducing and stabilizing agents during nanoparticle synthesis. These biomolecules facilitate the conversion of Zn^{2+} ions into ZnO nanoparticles and prevent aggregation. [37–39].

3.2. Characterization of Df-ZnO NPs

3.2.1. UV-Visible-

The UV–Visible absorption spectrum of ZnO nanoparticles synthesized using *Dolichandrone falcata* plant extract by the green synthesis method is shown in the figure. The spectrum exhibits a strong and well-defined absorption peak at around **360 nm**, which is characteristic of ZnO nanoparticles and corresponds to their intrinsic band gap absorption due to electron transition from the valence band to the conduction band[41]. The appearance of this absorption peak confirms the successful formation of ZnO nanoparticles. The slight broadening of the peak indicates nanoscale particle size and possible size distribution of the synthesized nanoparticles. The absorption in the UV region also suggests good optical properties of ZnO NPs, which are desirable for applications in photocatalysis, antimicrobial activity, and optoelectronic devices. The use of *D. falcata* extract likely played a dual role as a reducing as well as stabilizing agent, facilitating nanoparticle formation without the use of toxic chemicals [40]. Overall, the UV–Vis analysis confirms the successful green synthesis of ZnO nanoparticles using *Dolichandrone falcata* plant extract.

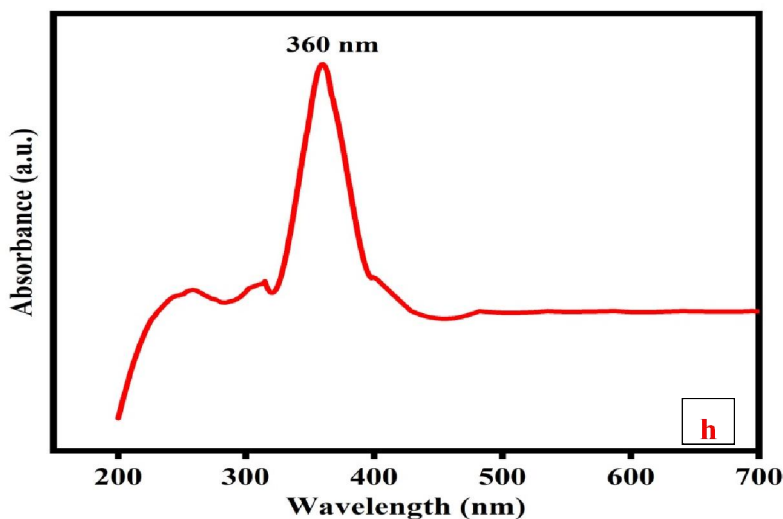


Figure 1: UV–Visible absorption spectrum of Df–ZnO nanoparticles.

3.2.2 Infrared analysis of Df-ZnO NPs:

The FTIR spectrum of ZnO nanoparticles synthesized using *Dolichandrone falcata* plant extract by the green synthesis method confirms the formation of ZnO and the involvement of plant phytochemicals in nanoparticle synthesis. A broad absorption band observed in the region of 3442 cm^{-1} corresponds to O–H stretching vibrations, indicating the presence of hydroxyl groups from phenols, alcohols, or adsorbed moisture. These functional groups from the plant extract are likely responsible for the reduction and stabilization of ZnO nanoparticles. The absorption bands around 1640 cm^{-1} can be attributed to C=O or N–H bending vibrations, suggesting the presence of proteins or other biomolecules acting as capping agents. Peaks observed in the region of $1400\text{--}1500\text{ cm}^{-1}$ are associated with C–H bending or aromatic ring



vibrations, further supporting the role of phytoconstituents in nanoparticle stabilization. A strong and characteristic absorption band in the low wavenumber region around 444 cm^{-1} corresponds to Zn–O stretching vibrations, confirming the successful formation of ZnO nanoparticles[42]. Overall, the FTIR analysis demonstrates that biomolecules present in *D. falcata* extract effectively participated in the green synthesis, acting as reducing and stabilizing agents, leading to the formation of stable ZnO nanoparticles suitable for biological and environmental applications[43].

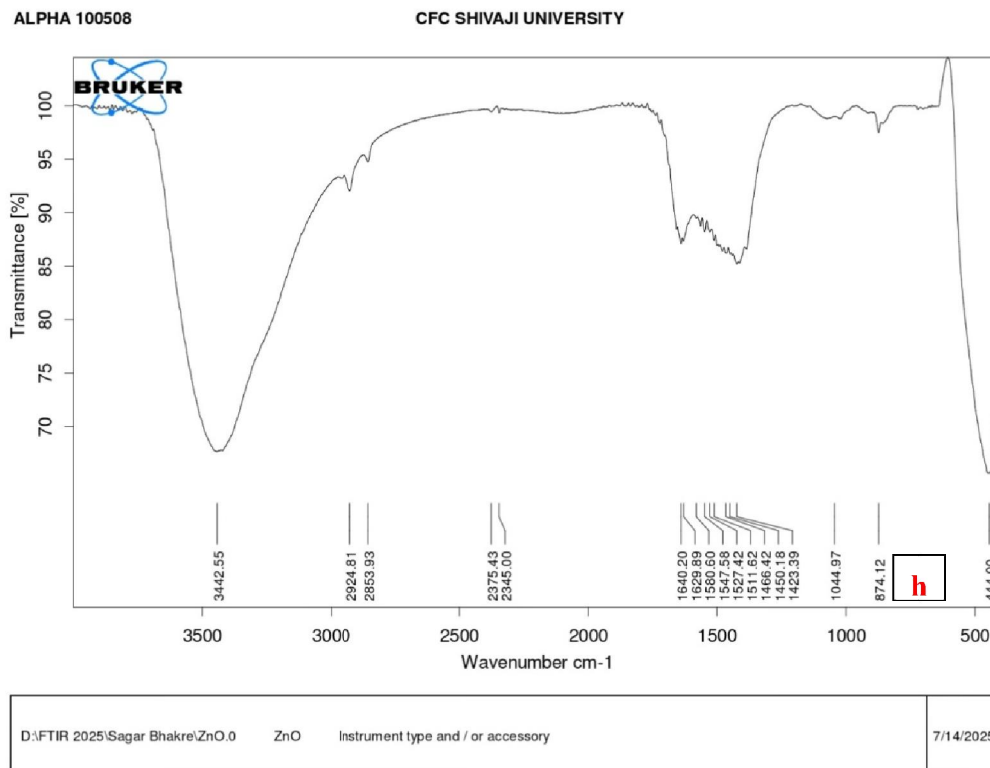


Figure 2: FTIR absorption spectrum of Df–ZnO nanoparticles showing characteristic vibrational frequencies.

3.2.3. X-ray Diffraction

The crystalline structure and phase purity of ZnO nanoparticles synthesized using *Dolichandrone falcata* plant extract were analyzed by X-ray diffraction (XRD). The diffraction pattern recorded in the 2θ range of 10° – 90° exhibits sharp and intense peaks, confirming the formation of highly crystalline ZnO nanoparticles.

The diffraction peaks observed at 2θ values of approximately 31.7° , 34.4° , 36.2° , 47.5° , 56.6° , 62.8° , 66.3° , 67.9° , and 69.1° correspond to the (100), (002), (101), (102), (110), (103), (200), **(112)**, and **(201)** planes, respectively. These reflections match well with the standard hexagonal wurtzite structure of ZnO (JCPDS No. 36-1451, space group $P6_3mc$). The absence of secondary or impurity peaks confirms the high phase purity of the biosynthesized nanoparticles.

The (101) reflection shows the highest intensity, indicating preferential orientation along this plane, which is characteristic of thermodynamically stable wurtzite ZnO[44]. The noticeable broadening of diffraction peaks compared to bulk ZnO suggests the formation of nanocrystalline particles. The average crystallite size was estimated using the Debye–Scherrer equation based on the (101) peak, yielding a crystallite size in the nanometer range (30 nm). The reduced crystallite size is attributed to the presence of bioactive phytochemicals in the *Dolichandrone falcata* extract, which act as natural reducing and capping agents, effectively controlling crystal growth and preventing agglomeration.



Overall, the XRD results confirm the successful green synthesis of phase-pure, highly crystalline hexagonal ZnO nanoparticles, demonstrating that *Dolichandrone falcata* extract is an efficient biotemplate for producing structurally stable ZnO nanomaterials suitable for advanced functional applications.

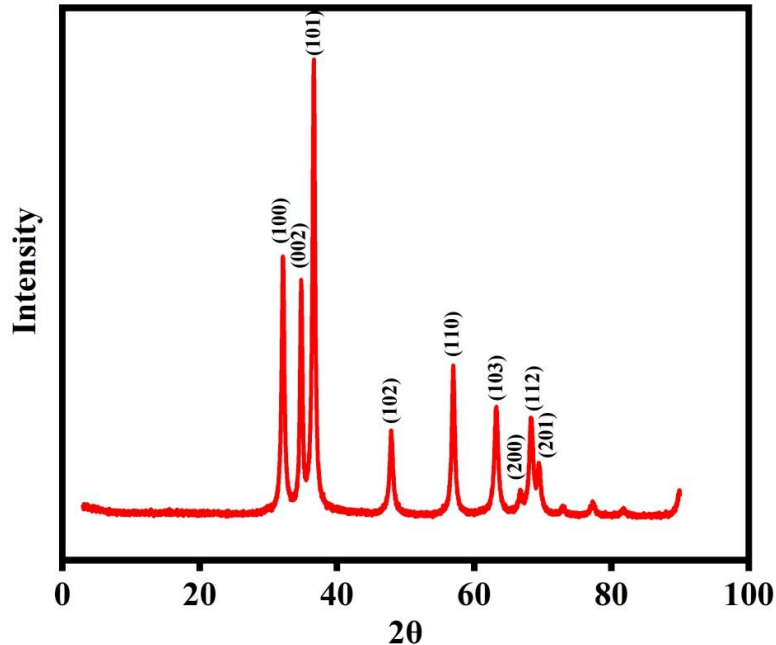


Figure 3: XRD pattern of Df-ZnO nanoparticles showing characteristic diffraction peaks

3.2.4 Scanning Electron Microscopy-

The surface morphology of the biosynthesized ZnO nanoparticles was examined using scanning electron microscopy (SEM) at different magnifications. The SEM micrographs reveal that the ZnO nanoparticles are irregularly shaped and highly agglomerated, forming cluster-like structures. Such agglomeration is commonly observed in metal oxide nanoparticles due to their high surface energy and strong interparticle interactions. At lower magnification, the particles appear as dense aggregates distributed uniformly over the surface, while higher magnification images show that these aggregates are composed of fine nanosized primary particles. The individual nanoparticles are not distinctly separated, indicating that the particles are loosely bound together, likely through phytochemical residues from the *Dolichandrone falcata* extract acting as capping agents during synthesis. The observed agglomeration supports the XRD results, which confirmed the nanocrystalline nature of ZnO. The formation of clustered structures may enhance surface roughness and increase the effective surface area, which is advantageous for applications such as photocatalysis and antimicrobial activity.

Overall, the SEM analysis confirms the successful green synthesis of ZnO nanoparticles with nanostructured morphology, demonstrating that *Dolichandrone falcata* plant extract plays a significant role in controlling particle formation and stabilization.



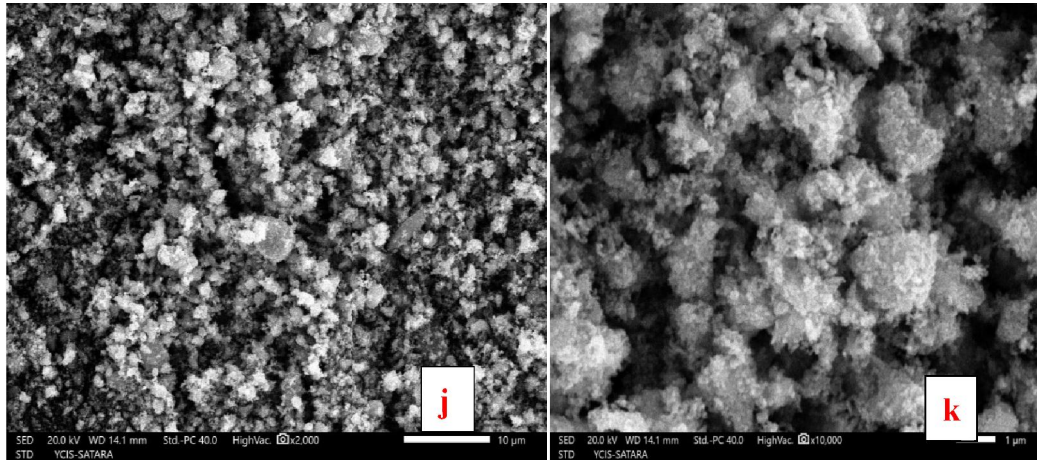


Figure 4: SEM images (j, k) of Df-ZnO nanoparticles at different magnifications.

3.2.5 EDAX

The elemental composition and purity of the biosynthesized ZnO nanoparticles were confirmed using energy-dispersive X-ray analysis (EDAX). The EDAX spectrum shows prominent peaks corresponding to zinc (Zn) and oxygen (O), confirming the successful formation of ZnO nanoparticles. Quantitative analysis reveals that Zn and O are the major elements present, with atomic percentages of approximately 45.18% for Zn and 54.82% for O, which is close to the stoichiometric ratio expected for ZnO. The corresponding weight percentages were found to be 77.11% Zn and 22.89% O, further validating the composition of zinc oxide.

Minor signals corresponding to carbon (C) and copper (Cu) were also detected. The presence of carbon is attributed to residual phytochemicals from the *Dolichandrone falcata* plant extract that act as natural capping and stabilizing agents during green synthesis. The copper signal is likely due to the sample holder or grid used during SEM-EDAX analysis rather than intrinsic contamination. The absence of additional elemental peaks confirms the **high purity** of the synthesized ZnO nanoparticles. Overall, the EDAX results strongly support the XRD and SEM findings, demonstrating that the green synthesis route using *Dolichandrone falcata* extract produces chemically pure and stoichiometrically consistent ZnO nanoparticles, suitable for various functional applications.



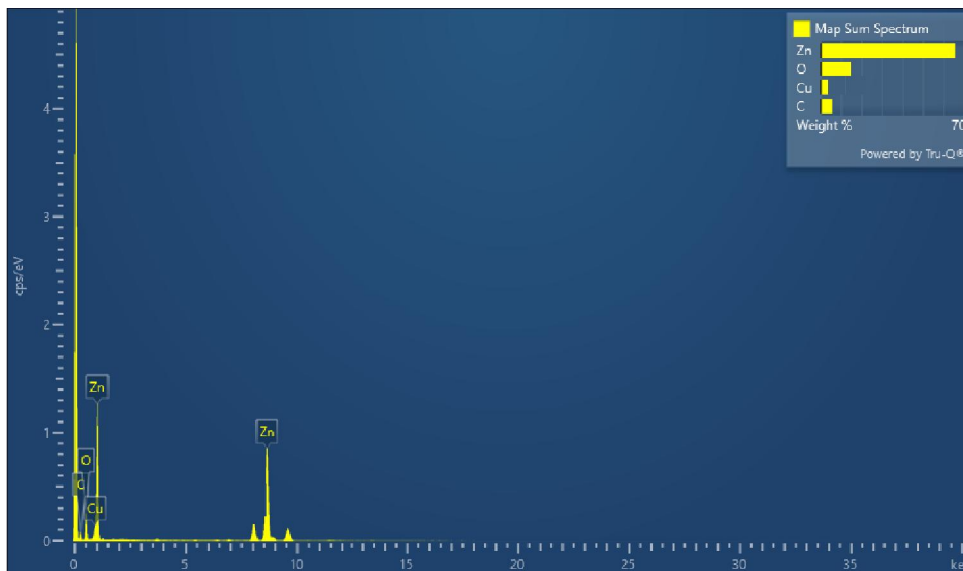


Figure 5: EDAX spectrum of Df-ZnO nanoparticles showing elemental composition.

3.2.6 Transmission Electron Microscopy:

Transmission electron microscopy (TEM) was used to analyze the morphology and particle size of ZnO nanoparticles synthesized using *Dolichandrone falcata* plant extract. The TEM images show that the nanoparticles are predominantly quasi-spherical to hexagonal in shape and moderately agglomerated, which is typical for ZnO nanoparticles due to high surface energy. The particle size distribution indicates that the ZnO nanoparticles are in the range of approximately 20–40 nm, with an average size around ~30 nm. This particle size is in good agreement with the crystallite size estimated from XRD analysis, confirming the nanocrystalline nature of the material. The clear particle boundaries and uniform contrast observed in the images indicate good crystallinity, while slight agglomeration is attributed to phytochemical capping from the plant extract[45].

Overall, the TEM results confirm the successful green synthesis of nanosized, crystalline ZnO nanoparticles, demonstrating the effectiveness of *Dolichandrone falcata* extract in controlling particle growth.

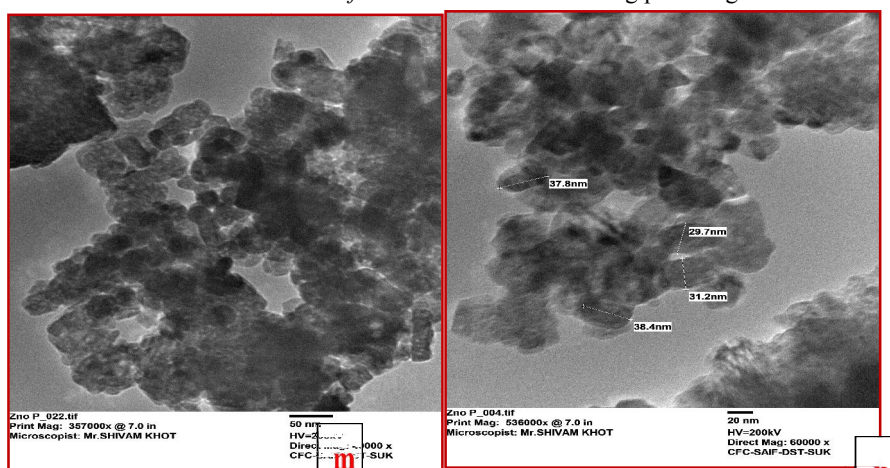


Figure 6: TEM images (m, n) of Df-ZnO nanoparticles at different magnifications.



3.2.7. Particle Size Distribution:

The particle size distribution of ZnO nanoparticles synthesized using *Dolichandrone falcata* plant extract was evaluated by DLS. The analysis showed a single dominant intensity peak, indicating a nearly monodisperse system. The Z-average particle size was 31.43 nm, while the main intensity peak was observed at 48.10 nm, confirming the formation of nanoparticles in the nanoscale range.

The polydispersity index (PDI) of 0.282 suggests a fairly narrow size distribution with limited aggregation. The good intercept value (0.892) reflects reliable measurement quality. The slightly larger hydrodynamic size is attributed to surface-bound phytochemicals from the plant extract, which act as capping and stabilizing agents. These results confirm the successful green synthesis of stable ZnO nanoparticles suitable for further applications.

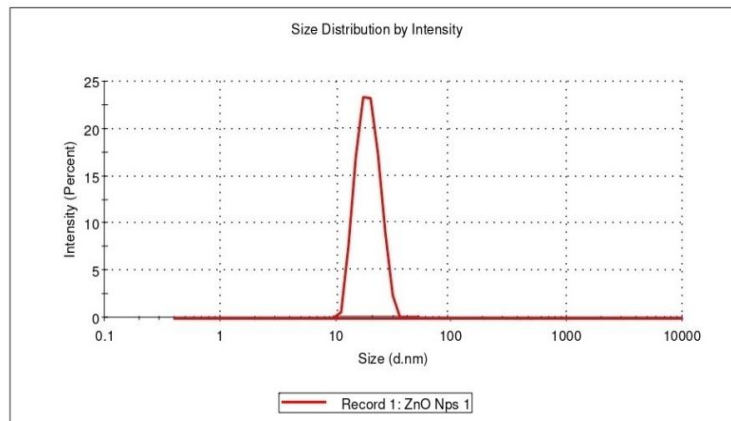


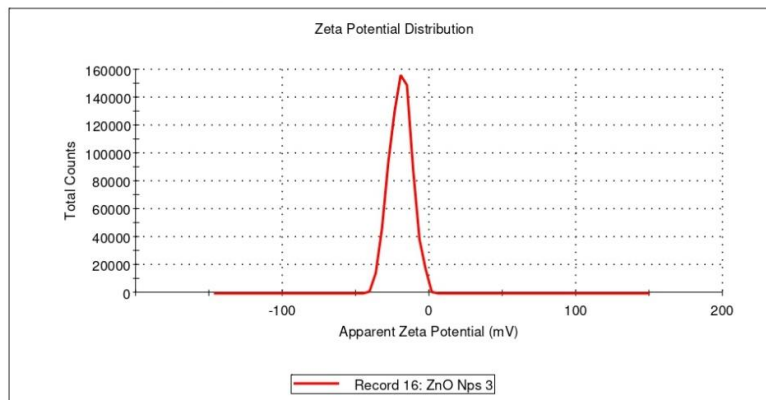
Figure 7: Particle size distribution graph of Df-ZnO nanoparticles.

3.2.8. Zeta Potential :

The zeta potential measurement of ZnO nanoparticles synthesized using *Dolichandrone falcata* plant extract showed a single dominant peak with a mean zeta potential value of **-19.6 mV**. This negative surface charge indicates the adsorption of phytochemicals from the plant extract on the nanoparticle surface, which act as natural capping agents[46].

The obtained zeta potential value suggests **moderate colloidal stability**, arising from electrostatic repulsion between particles that helps prevent rapid aggregation. The narrow peak distribution and good result quality further confirm the uniform surface charge of the nanoparticles. Although values above ± 30 mV indicate high stability, the observed -19.6 mV is typical for green-synthesized nanoparticles and is sufficient for short-term stability in aqueous media. Overall, the zeta potential results support the successful green synthesis and stabilization of ZnO nanoparticles using *Dolichandrone falcata* extract.





Malvern Instruments Ltd
www.malvern.com

Zetasizer Ver. 7.11
Serial Number : MAL1140144

File name: ZnO Nps.dts
Record Number: 16
25 Jul 2025 4:43:53 PM

Figure 8: Zeta potential of Df–ZnO nanoparticles.

3.2.9. X-ray Photo electron Spectroscopy

X-ray photoelectron spectroscopy (XPS) analysis was carried out to determine the surface elemental composition and chemical states of zinc oxide nanoparticles synthesized using *Dolichandrone falcata* plant extract. The wide-scan XPS spectrum confirms the presence of Zn, O, and C without any extraneous impurity peaks, indicating the formation of chemically pure ZnO nanoparticles. The survey spectrum displays characteristic peaks corresponding to Zn 2p, Zn 3s, Zn 3p, Zn 2s, O 1s, and C 1s. The C 1s peak observed at a binding energy of ~284.6 eV is attributed to adventitious carbon and organic phytochemicals from the plant extract adsorbed on the nanoparticle surface, which act as capping and stabilizing agents. The high-resolution Zn 2p spectrum exhibits two prominent peaks at binding energies of approximately 1021.6–1022.0 eV (Zn 2p_{3/2}) and 1044.6–1045.0 eV (Zn 2p_{1/2}), with a spin–orbit splitting of ~23 eV. These values are characteristic of Zn²⁺ ions in the ZnO lattice, confirming the oxidation state of zinc and the absence of metallic Zn or other zinc sub-oxides.

The O 1s core-level spectrum shows a dominant peak centered at ~530.0–530.2 eV, which corresponds to lattice oxygen (O²⁻) in ZnO. A weak shoulder at higher binding energy (~531.5–532.0 eV) can be ascribed to surface hydroxyl groups or adsorbed oxygen species, commonly observed in green-synthesized metal oxide nanoparticles due to residual organic compounds.

Quantitative XPS analysis reveals atomic percentages of Zn (38.81%), O (31.69%), and C (29.51%). The Zn/O ratio is close to the stoichiometric composition of ZnO, confirming successful oxide formation. The relatively high carbon content further supports the involvement of *Dolichandrone falcata* phytochemicals in surface functionalization and stabilization of the nanoparticles.

Overall, the XPS results confirm the formation of ZnO nanoparticles with Zn²⁺ oxidation state and well-defined lattice oxygen, while the presence of surface-bound organic species highlights the effectiveness of the plant extract in green synthesis which is in accordance with previously reported work [47].



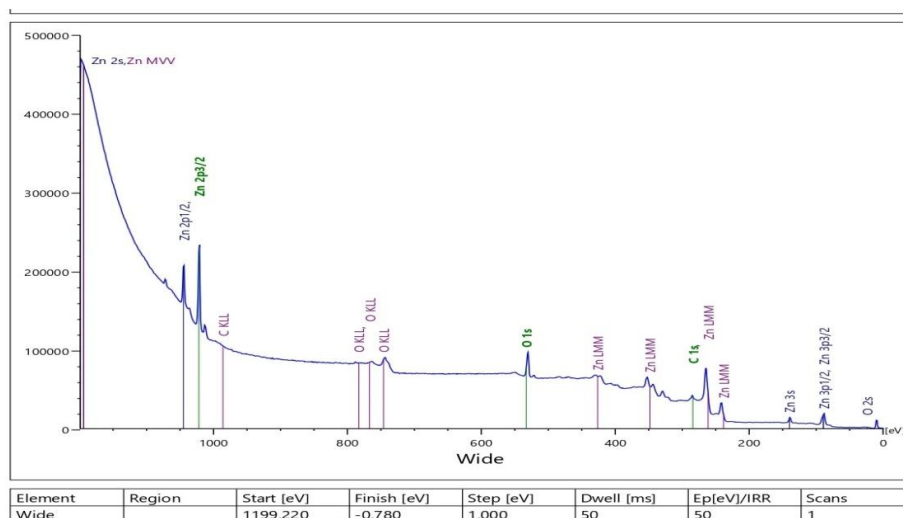


Figure 9: XPS qualitative spectrum of Df-ZnO nanoparticles.

3.3 Biological Activities

3.3.1 Antibacterial Activity:

The antibacterial activity of zinc oxide nanoparticles (ZnO-1) was evaluated using the agar well diffusion method against *Streptococcus pneumoniae* (ATCC 6303) and *Xanthomonas citri* (ATCC 19315). Streptomycin (1 mg/mL) was used as a positive control, while dimethyl sulfoxide (DMSO) served as a negative control. All experiments were conducted in triplicate, and results are expressed as mean zone of inhibition (ZOI) ± standard deviation (SD).

ZnO-1 nanoparticles exhibited pronounced antibacterial activity against both tested strains, whereas no inhibition was observed for the negative control, confirming the absence of solvent effects. Against *S. pneumoniae*, ZnO-1 produced a ZOI of **21.0 ± 0.0 mm**, compared to **28.0 ± 0.0 mm** for Streptomycin. Similarly, ZnO-1 showed a ZOI of **21.0 ± 0.0 mm** against *X. citri*, while the standard drug exhibited **25.0 ± 0.0 mm** inhibition.

The antibacterial efficacy of ZnO nanoparticles is primarily attributed to their ability to generate reactive oxygen species, disrupt bacterial membrane integrity, and interact with intracellular biomolecules, leading to cell damage and growth inhibition[48]. Although ZnO-1 demonstrated slightly lower activity than Streptomycin, its strong antibacterial performance, combined with favorable biointerface properties such as stability and biocompatibility, highlights its potential for biomedical and antimicrobial surface applications

Table 1: Antibacterial activity of ZnO nanoparticles against Gram-positive and Gram-negative bacteria.

Sample	Concentration (µg mL ⁻¹)	Zone of inhibition (mm) <i>S. pneumoniae</i>	Zone of inhibition (mm) – <i>X. citri</i>
Control (DMSO)	40	00	00
Streptomycin (Standard)	40	28± 0.1	25± 0.2
ZnO-1 nanoparticles	40	21± 1.0	21± 0.3

Values represent mean inhibition zones measured by agar well diffusion assay



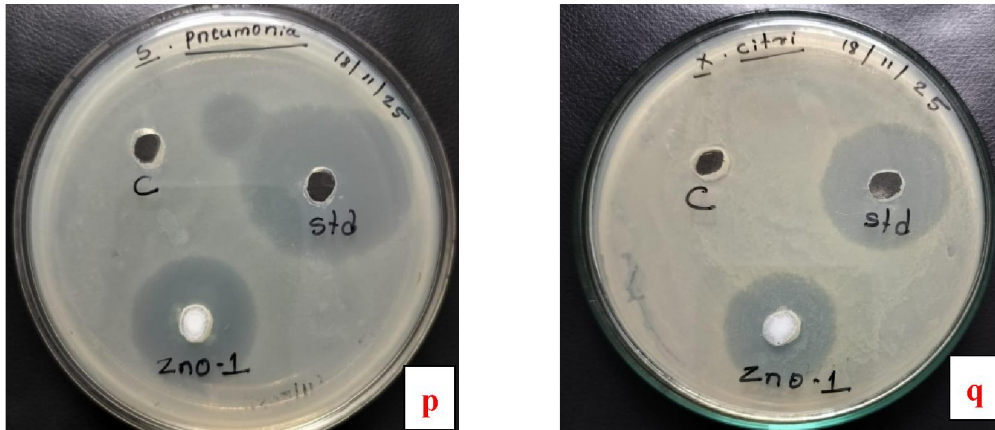


Figure 10: Images (p, q) showing the antibacterial activity of Df-ZnO nanoparticles against Gram-positive and Gram-negative bacteria.

3.3.2 Antifungal Activity of Df-ZnO NPs:

The antifungal activity of synthesized zinc oxide nanoparticles (ZnO-1) was assessed using the agar well diffusion method against *Aspergillus niger* (ATCC 9029) and *Aspergillus alternata* (ATCC 66981). Miconazole (1 mg/mL) and DMSO were used as positive and negative controls, respectively. All assays were performed in triplicate, and results were expressed as mean zone of inhibition (ZOI) \pm SD.

ZnO-1 exhibited moderate antifungal activity against both fungal strains, while no inhibition was observed for the negative control. Against *A. niger*, ZnO-1 produced a ZOI of 9.0 ± 0.0 mm compared to 23.0 ± 0.0 mm for Miconazole. Similarly, a ZOI of 6.0 ± 0.0 mm was observed against *A. alternata*, whereas the standard drug showed 22.0 ± 0.0 mm inhibition.

The antifungal efficacy of ZnO nanoparticles is attributed to reactive oxygen species generation, membrane disruption, and interactions with intracellular biomolecules, leading to fungal growth inhibition. Although ZnO-1 showed lower activity than Miconazole, its stability, biocompatibility, and reduced risk of resistance highlight its potential as an alternative or adjunct antifungal agent.

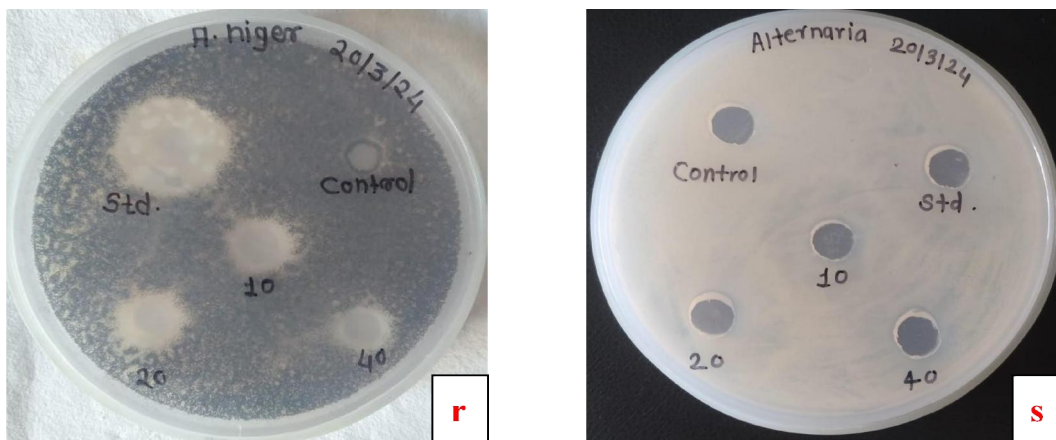


Figure 11: Images (r, s) showing the antifungal activity of Df-ZnO nanoparticles against *Aspergillus niger* and *Alternaria* species.



Table 2: Antifungal activity of ZnO nanoparticles against *Aspergillus niger* and *Alternaria alternata*.

Sample	Zone of inhibition (mm) – <i>A. niger</i>	Zone of inhibition (mm) – <i>A. alternata</i>
Control (DMSO)	0.0 ± 0.0	0.0 ± 0.0
Miconazole (1 mg/mL)	23.0 ± 0.2	22.0 ± 1.0
ZnO-1	9.0 ± 0.4	6.0 ± 0.2

Values represent mean ± SD (n = 3).

3.3.3 Antioxidant Activity by DPPH assay:

The free radical scavenging potential of ZnO nanoparticles (ZnO-1) was evaluated by the DPPH assay at concentrations ranging from 20 to 100 µg/mL, using ascorbic acid as a positive control. ZnO-1 exhibited a marked concentration-dependent antioxidant response, with inhibition values increasing from 14.50% to 62.17% as the concentration increased. This trend indicates enhanced interaction between ZnO nanoparticles and DPPH radicals at higher doses.

Table 3: Antioxidant activity of ZnO nanoparticles determined by the DPPH assay.

Sr.No	Sample Code	Concentration (µg/ml)	Absorbance at 510nm				Inhibition (%)	IC ₅₀ (µg/ml)
			Test 1	Test 2	Test 3	Mean		
1	Control	-	1.93	1.93	1.93	1.93	-	
2	Standard (Ascorbic Acid)	20	1.45	1.42	1.40	1.42	26.42%	72.49
		40	1.31	1.29	1.33	1.31	32.12%	
		60	0.95	0.97	0.93	0.95	50.77%	
		80	0.82	0.85	0.79	0.82	57.51%	
		100	0.35	0.32	0.32	0.33	82.90%	
3	ZnO-1	20	1.62	1.65	1.68	1.65	14.50%	78.71
		40	1.45	1.50	1.55	1.50	22.27%	
		60	1.16	1.19	1.22	1.19	38.34%	
		80	0.92	0.94	0.98	0.94	51.29%	
		100	0.71	0.74	0.74	0.73	62.17%	

The IC₅₀ value of ZnO-1 (78.71 µg/mL) was found to be close to that of ascorbic acid (72.49 µg/mL), suggesting moderate to strong antioxidant activity. The observed scavenging performance may be attributed to surface-mediated redox reactions and the availability of active sites on ZnO nanoparticles, which promote efficient electron or hydrogen transfer[49]. Present findings highlight the suitability of ZnO-1 nanoparticles as potential antioxidant agents, supporting their further investigation in drug delivery and biomedical applications.

3.3.4 In vitro anti-inflammatory activity by Protein denaturation method:

The anti-inflammatory activity of ZnO nanoparticles (ZnO-1) was assessed using the protein denaturation assay, a well-established in vitro model for preliminary screening of anti-inflammatory potential. ZnO-1 exhibited a concentration-dependent inhibition of protein denaturation over the tested range of 20–100 µg/mL. The inhibition increased from 5.84% at 20 µg/mL to 43.50% at 100 µg/mL, indicating a gradual enhancement of anti-inflammatory response with increasing nanoparticle concentration.

Diclofenac sodium, used as the reference standard, showed markedly higher inhibition at all concentrations, confirming the sensitivity and validity of the assay. In comparison, ZnO-1 demonstrated moderate inhibitory activity, particularly



at higher concentrations, suggesting partial protection against thermally induced protein denaturation. The observed effect may be associated with surface-mediated interactions of ZnO nanoparticles that contribute to protein stabilization and attenuation of denaturation processes. However, the lower efficacy relative to the standard drug indicates that the anti-inflammatory potential of ZnO-1 is limited under the present experimental conditions.

Overall, these results suggest that ZnO-1 nanoparticles possess measurable but moderate in vitro anti-inflammatory activity, warranting further mechanistic investigations and in vivo validation to clarify their relevance in inflammation-related biomedical applications.

Table 4: *In vitro* anti-inflammatory activity of ZnO nanoparticles assessed by the protein denaturation method.

Protein denaturation assay								
SR. NO	Sample code	Concentration (µg/ml)	Absorbance at 660nm				% Inhibition	IC50 (µg/ml)
			Test 1	Test 2	Test 3	Mean		
1	Control		1.54	1.54	1.54	1.54	-	
2	Standard (Diclofenac Sodium)	20	1.40	1.37	1.39	1.32	16.98%	70.91
		40	1.20	1.20	1.22	1.20	24.52%	
		60	0.96	0.97	0.98	0.91	42.76%	
		80	0.72	0.72	0.71	0.65	59.11%	
		100	0.42	0.45	0.44	0.21	86.79%	
3	ZnO-1	20	1.49	1.46	1.42	1.45	5.84%	NE
		40	1.35	1.33	1.32	1.33	13.63%	
		60	1.21	1.23	1.20	1.21	21.42%	
		80	1.03	1.05	1.02	1.03	33.11%	
		100	0.88	0.88	0.86	0.87	43.50%	

4. Conclusion: In the present study, zinc oxide nanoparticles (ZnO NPs) were successfully synthesized via an eco-friendly green route using *Dolichandrone falcata* leaf extract, demonstrating an effective and sustainable alternative to conventional chemical methods. The phytochemical constituents of the plant extract played a dual role as reducing and stabilizing agents, facilitating the formation of stable and well-defined nanoparticles.

Comprehensive characterization using UV-Visible spectroscopy, FTIR, XRD, SEM, TEM, EDAX, DLS, zeta potential, and XPS confirmed the successful formation of crystalline, phase-pure ZnO nanoparticles with nanoscale dimensions (~30 nm), hexagonal wurtzite structure, and moderate colloidal stability. The presence of surface-bound phytochemicals further contributed to nanoparticle stabilization and functionalization.

Biological evaluations revealed that the synthesized ZnO nanoparticles exhibit significant antibacterial activity against *Streptococcus pneumoniae* and *Xanthomonas citri*, along with moderate antifungal activity against *Aspergillus niger* and *Alternaria alternata*. The nanoparticles also demonstrated concentration-dependent antioxidant activity with appreciable free radical scavenging potential, as well as moderate anti-inflammatory effects through inhibition of protein denaturation. These biological properties are primarily attributed to reactive oxygen species (ROS) generation, surface reactivity, and interactions with microbial and cellular components.

Overall, the findings of this study highlight that plant-mediated ZnO nanoparticles possess multifunctional properties and hold considerable promise for applications in antimicrobial formulations, antioxidant systems, and biomedical research. Furthermore, the green synthesis approach offers advantages such as cost-effectiveness, environmental compatibility, and scalability. Future investigations focusing on in vivo studies, toxicity assessment, and mechanistic insights will further establish their potential for clinical and industrial applications.



Credit authorship contribution statement

Sagar D. Bhakare: Conceptualization, Writing - original draft, Writing - review & editing; Sudhir B. Kumbhar: Methodology, Formal analysis; Dilip D. Anuse: Formal analysis, Investigation, Validation; Dr. Santosh B. Gaikwad: Formal analysis & editing.

Funding

This research work has been funded by Pradhan Mantri Uchchar Shiksha Abhiyan (PM-USHA), Government of India.

Acknowledgment

The authors thank the Department of Chemistry Dahiwadi College, Dahiwadi Dist. Satara for providing a laboratory facility. The authors also thank the Pradhan Mantri Uchchar Shiksha Abhiyan (PM-USHA), Government of India. The authors are thankful to Infinite Biotech Institute Research and Analytics, Sangali, for availing the characterization, antimicrobial, and anti-inflammatory anti-oxidant activity.

Abbreviations

The following abbreviations are used in this manuscript:

ZnO NPs	Zinc Oxide Nanoparticles
Df-ZnO NPs	<i>Dolichandrone Falcata</i> -Mediated Copper Oxide Nanoparticles
M-M	Metal-Metal
M-O	Metal-Oxygen
gm	Gram
°C	Degree Celsius
µg	Microgram
mg	Milligram
nm	Nanometer
µm	Micrometer
mm	Milli meter
DMSO	Dimethyl sulfoxide
ppm	Parts Per Million
MIC	Minimum Inhibitory Concentration
RT	Room Temperature
mmol	Milli Mole
hrs	Hours
µL/mL	Micro Litre/Milli Litre
UV-Vis	Ultraviolet-Visible Absorption Spectroscopy
TEM	Transmission Electron Microscopy
SEM	Scanning Electron Microscopy
XRD	X-Ray Diffraction
IC	Inhibitory Concentration
EDX	Energy Dispersive X-ray Spectroscopy
OD	Optical Density
PBS	Phosphate Buffered Saline
ROS	Reactive Oxygen Species
RNS	Reactive Nitrogen Species



REFERENCES

- [1] S. Bayda, M. Adeel, T. Tuccinardi, M. Cordani, and F. Rizzolio, "The History of Nanoscience and Nanotechnology: From Chemical–Physical Applications to Nanomedicine," *Molecules*, vol. 25, no. 1, p. 112, Dec. 2019, doi: 10.3390/molecules25010112.
- [2] O. O. Ogochukwu, M. B. Fabiyi, O. S. Aworunse, O. A. Oyewole, and P. O. Isibor, "Nanoparticle Properties and Characterization," *Environ. Nanotoxicology Combat. Minute Contam.*, pp. 23–40, Mar. 2024, doi: 10.1007/978-3-031-54154-4_2.
- [3] D. J. G. Dabodabo and C. J. H. Solidor, "Metal Oxide Nanoparticles for Various Applications," *Carrageenan-Mediated Green Synth. Met. Oxide Nanoparticles Var. Appl.*, pp. 84–101, Jan. 2025, doi: 10.1201/9781003610229-5/
- [4] P. Kumar, S. Kaushal, S. Kumar, J. Dalal, K. M. Batoo, and D. S. Ahlawat, "Recent advancements in pure and doped zinc oxide nanostructures for UV photodetectors application," *Phys. B Condens. Matter*, vol. 707, p. 417177, Jun. 2025, doi: 10.1016/J.PHYSB.2025.417177.
- [5] R. Ghamarpoor, A. Fallah, and M. Jamshidi, "Investigating the use of titanium dioxide (TiO₂) nanoparticles on the amount of protection against UV irradiation," *Sci. Reports 2023 131*, vol. 13, no. 1, pp. 9793–, Jun. 2023, doi: 10.1038/s41598-023-37057-5.
- [6] R. Rafi *et al.*, "Smart wound dressings based on carbon doped copper nanoparticles for selective bacterial detection and eradication for efficient wound healing application," *Mater. Today Commun.*, vol. 35, p. 105914, Jun. 2023, doi: 10.1016/J.MTCOMM.2023.105914.
- [7] M. Rahman, "Magnetic Resonance Imaging and Iron-oxide Nanoparticles in the era of Personalized Medicine," *Nanotheranostics*, vol. 7, no. 4, p. 424, 2023, doi: 10.7150/NTNO.86467.
- [8] S. Mohammed Fayyadh and A. Ben Ahmed, "A comparative study between the use of nanoparticles of magnesium oxide and zinc oxide as coating for polymeric surfaces a flame retardant and corrosion resistance," *Mater. Chem. Phys.*, vol. 314, p. 128899, Feb. 2024, doi: 10.1016/J.MATCHEMPHYS.2024.128899.
- [9] K. Nagaraj *et al.*, "Photocatalytic advancements and applications of titanium dioxide (TiO₂): Progress in biomedical, environmental, and energy sustainability," *Next Res.*, vol. 2, no. 1, p. 100180, Mar. 2025, doi: 10.1016/J.NEXRES.2025.100180.
- [10] A. Manuja *et al.*, "Metal/metal oxide nanoparticles: Toxicity concerns associated with their physical state and remediation for biomedical applications," *Toxicol. Reports*, vol. 8, pp. 1970–1978, Jan. 2021, doi: 10.1016/J.TOXREP.2021.11.020.
- [11] S. Palagati *et al.*, "Advanced Materials Synthesis by Top--Down and Bottom--Up Approaches," *Adv. Mater. Prod. Charact. Multidiscip. Appl.*, pp. 201–221, Jan. 2024, doi: 10.1201/9781003451198-10
- [12] F. Chen, T. H. Yan, S. Bashir, and J. L. Liu, "Synthesis of nanomaterials using top-down methods," *Adv. Nanomater. Their Appl. Renew. Energy, Second Ed.*, pp. 37–60, Jan. 2022, doi: 10.1016/B978-0-323-99877-2.00007-2.
- [13] A. Biswas, I. S. Bayer, A. S. Biris, T. Wang, E. Dervishi, and F. Faupel, "Advances in top–down and bottom–up surface nanofabrication: Techniques, applications & future prospects," *Adv. Colloid Interface Sci.*, vol. 170, no. 1–2, pp. 2–27, Jan. 2012, doi: 10.1016/J.CIS.2011.11.001.
- [14] K. Hachem *et al.*, "Methods of Chemical Synthesis in the Synthesis of Nanomaterial and Nanoparticles by the Chemical Deposition Method: A Review," *BioNanoScience 2022 123*, vol. 12, no. 3, pp. 1032–1057, Jun. 2022, doi: 10.1007/S12668-022-00996-W.
- [15] S. K. Gore, S. S. Jadhav, U. B. Tumberphale, and S. D. Raut, "Sol-gel technology for the synthesis of metal oxide nanostructures," *Solut. Methods Met. Oxide Nanostructures*, pp. 19–38, Jan. 2023, doi: 10.1016/B978-0-12-824353-4.00011-7.
- [16] E. M. Abdel-Fattah *et al.*, "Hydrothermal Synthesis of ZnO Nanoflowers: Exploring the Relationship between Morphology, Defects, and Photocatalytic Activity," *Cryst. 2024, Vol. 14*, vol. 14, no. 10, Oct. 2024, doi:



- 10.3390/CRYST14100892.
- [17] S. O. Badmus, H. K. Amusa, T. A. Oyehan, and T. A. Saleh, "Environmental risks and toxicity of surfactants: overview of analysis, assessment, and remediation techniques," *Environ. Sci. Pollut. Res.* 2021 2844, vol. 28, no. 44, pp. 62085–62104, Sep. 2021, doi: 10.1007/S11356-021-16483-W.
- [18] A. Khlyustova, Y. Cheng, and R. Yang, "Vapor-deposited functional polymer thin films in biological applications," *J. Mater. Chem. B*, vol. 8, no. 31, pp. 6588–6609, Aug. 2020, doi: 10.1039/D0TB00681E.
- [19] M. Pirsaeheb *et al.*, "Green synthesis of nanomaterials by using plant extracts as reducing and capping agents," *Environ. Sci. Pollut. Res.* 2024 3117, vol. 31, no. 17, pp. 24768–24787, Mar. 2024, doi: 10.1007/S11356-024-32983-X.
- [20] J. Pathak *et al.*, "Exploring the Paradigm of Phyto-Nanofabricated Metal Oxide Nanoparticles: Recent Advancements, Applications, and Challenges," *Mol. Biotechnol.* 2023, pp. 1–21, Jul. 2023, doi: 10.1007/S12033-023-00799-8.
- [21] S. S. Chowdhury, N. Ibbat, M. Hasan, and A. Ghosh, "Medicinal Plant-Based Nanoparticle Synthesis and their Diverse Applications," *Ethnopharmacol. Omi. Adv. Med. Plants Vol. 2 Reveal. Secrets Med. Plants*, pp. 213–250, Jan. 2024, doi: 10.1007/978-981-97-4292-9_10.
- [22] A. M. El-Khawaga, M. Orlandini, L. Raucchi, and K. Elmaghraby, "Magnetic nanoparticles as a promising antimicrobial agent for combating multidrug resistant bacteria: a review," *Discov. Appl. Sci.* 2025 77, vol. 7, no. 7, pp. 652–, Jun. 2025, doi: 10.1007/S42452-025-06601-5.
- [23] A. Sirelkhatim *et al.*, "Review on Zinc Oxide Nanoparticles: Antibacterial Activity and Toxicity Mechanism," *Nano-Micro Lett.* 2015 73, vol. 7, no. 3, pp. 219–242, Apr. 2015, doi: 10.1007/S40820-015-0040-X.
- [24] M. J. Mphahlele, G. K. More, M. M. Maluleka, and Y. S. Choong, "Bio-evaluation of the 2-nitrochalcones as potential anti-lung cancer agents, inducers of apoptosis and inhibitors of protein kinase (VEGFR-2)," *Med. Chem. Res.* 2023 3211, vol. 32, no. 11, pp. 2380–2393, Aug. 2023, doi: 10.1007/S00044-023-03136-5.
- [25] Y. Kiraz, A. Adan, M. Kartal Yandim, and Y. Baran, "Major apoptotic mechanisms and genes involved in apoptosis," *Tumor Biol.* 2016 377, vol. 37, no. 7, pp. 8471–8486, Apr. 2016, doi: 10.1007/S13277-016-5035-9.
- [26] K. A. Saraswathi *et al.*, "Zinc Oxide-Based Antibacterial and Anti-viral Functional Materials," *ACS Symp. Ser.*, vol. 1472, pp. 281–307, Jun. 2024, doi: 10.1021/BK-2024-1472.CH009.
- [27] N. A. El-Baky, A. A. A. F. Amara, N. A. El-Baky, and A. A. A. F. Amara, "Recent Approaches towards Control of Fungal Diseases in Plants: An Updated Review," *J. Fungi* 2021, Vol. 7, vol. 7, no. 11, Oct. 2021, doi: 10.3390/JOF7110900.
- [28] B. Akbari, N. Baghaei-Yazdi, M. Bahmaie, and F. Mahdavi Abhari, "The role of plant-derived natural antioxidants in reduction of oxidative stress," *Biofactors*, vol. 48, no. 3, pp. 611–633, May 2022, doi: 10.1002/biof.1831.
- [29] D. Laveti *et al.*, "Anti-Inflammatory Treatments for Chronic Diseases: A Review," *Inflamm. Allergy-Drug Targets*, vol. 12, no. 5, pp. 349–361, Sep. 2013, doi: 10.2174/18715281113129990053.
- [30] G. Kumar, V. Tomar, P. Kumar, and M. Nemiwal, "Zinc Oxide Nanoparticles as Efficient Heterogeneous Catalyst for Synthesis of Bio-active Heterocyclic Compounds," *ChemistrySelect*, vol. 8, no. 41, p. e202303181, Nov. 2023, doi: 10.1002/SLCT.202303181;ISSUE:ISSUE:DOI.
- [31] R. Shah and P. K. Verma, "Synthesis of thiophene derivatives and their anti-microbial, antioxidant, anticorrosion and anticancer activity," *BMC Chem.* 2019 131, vol. 13, no. 1, pp. 54–, Apr. 2019, doi: 10.1186/S13065-019-0569-8.
- [32] S. Raha and M. Ahmaruzzaman, "ZnO nanostructured materials and their potential applications: progress, challenges and perspectives," *Nanoscale Adv.*, vol. 4, no. 8, pp. 1868–1925, Apr. 2022, doi: 10.1039/D1NA00880C.
- [33] A. Hamidi and M. Poudineh, "Advancing Eco-friendly Biomedicine: Sustainable Nanocomposites as Platforms for Genetic Vaccines," pp. 303–356, 2025, doi: 10.1007/978-3-031-79110-9_11.



- [34] S. Daswadikar, M. Muley, S. Prasad, and P. Itankar, "Ethnobotanical and Conservational Studies of Medicinal Plants: A Case Study of *Dolichandrone falcata* (Wall. Ex DC.) Seem. in Western Ghats, India," *Ethnopharmacol. Omi. Adv. Med. Plants Uncovering Divers. Ethnopharmacol. Asp. Vol. 1*, pp. 103–113, Jan. 2024, doi: 10.1007/978-981-97-2367-6_6.
- [35] S. Dhaswadikar *et al.*, "Exploring the phytochemical and pharmacological insights of the plant *Dolichandrone falcata*," *Pharmacol. Res. - Nat. Prod.*, vol. 5, p. 100128, Dec. 2024, doi: 10.1016/J.PRENAP.2024.100128.
- [36] S. R. Dhaswadikar *et al.*, "Anti-hemorrhoidal potential of standardized leaf extract of *Dolichandrone falcata*," *Phytomedicine Plus*, vol. 2, no. 1, p. 100172, Feb. 2022, doi: 10.1016/J.PHYPLU.2021.100172.
- [37] "Phytochemical Methods A Guide to Modern Techniques of Plant Analysis | Springer Nature Link." Accessed: Feb. 20, 2026. [Online]. Available: <https://link.springer.com/book/9780412572609>
- [38] J. M. Al-Khayri, G. R. Sahana, P. Nagella, B. V. Joseph, F. M. Alessa, and M. Q. Al-Mssallem, "Flavonoids as Potential Anti-Inflammatory Molecules: A Review," *Mol. 2022, Vol. 27, Page 2901*, vol. 27, no. 9, p. 2901, May 2022, doi: 10.3390/molecules27092901.
- [39] S. Dhaswadikar *et al.*, "Exploring the phytochemical and pharmacological insights of the plant *Dolichandrone falcata*," *Pharmacol. Res. - Nat. Prod.*, vol. 5, p. 100128, Dec. 2024, doi: 10.1016/j.prenap.2024.100128.
- [40] W. Sun and M. H. Shahrajabian, "Therapeutic Potential of Phenolic Compounds in Medicinal Plants—Natural Health Products for Human Health," *Mol. 2023, Vol. 28, Page 1845*, vol. 28, no. 4, p. 1845, Feb. 2023, doi: 10.3390/molecules28041845.
- [41] R. S. Yadav, P. Mishra, and A. C. Pandey, "Growth mechanism and optical property of ZnO nanoparticles synthesized by sonochemical method," *Ultrason. Sonochem.*, vol. 15, no. 5, pp. 863–868, Jul. 2008, doi: 10.1016/j.ultsonch.2007.11.003.
- [42] A. Kolodziejczak-Radzimska and T. Jesionowski, "Zinc Oxide—From Synthesis to Application: A Review," *Mater. 2014, Vol. 7, Pages 2833-2881*, vol. 7, no. 4, pp. 2833–2881, Apr. 2014, doi: 10.3390/ma7042833.
- [43] S. Irvani, "Green synthesis of metal nanoparticles using plants," *Green Chem.*, vol. 13, no. 10, pp. 2638–2650, Jan. 2011, doi: 10.1039/c1gc15386b.
- [44] B. Flores, M. Guzman, O. Chumpitaz, S. Flores, A. Rodriguez, and J. E. Herrera, "Crystallographic and optical properties of ZnO nanoparticles prepared by two different methods," *Appl. Phys. A 2025 1314*, vol. 131, no. 4, pp. 300–, Mar. 2025, doi: 10.1007/s00339-025-08431-z.
- [45] M. Y. Al-darwesh, S. S. Ibrahim, and M. A. Mohammed, "A review on plant extract mediated green synthesis of zinc oxide nanoparticles and their biomedical applications," *Results Chem.*, vol. 7, no. 5, p. 101368, Jan. 2024, doi: 10.1016/j.rechem.2024.101368.
- [46] M. Y. Aysha, K. Selvam, R. Adhavan, P. Prakash, and M. S. Shivakumar, "Synthesis and Characterization of Chitosan-Zinc Oxide Nanocomposite for In Vitro Antibacterial, Anti-Inflammatory, Antioxidant and Anticancer Potential of *Dolichandrone falcata* (Wall. ex DC.) Seem. Leaf Extracts," *J. Clust. Sci. 2025 363*, vol. 36, no. 3, pp. 92–, Apr. 2025, doi: 10.1007/s10876-025-02812-3.
- [47] M. I. Selim, T. El-banna, F. Sonbol, and E. Elekhawy, "Arthrospira maxima and biosynthesized zinc oxide nanoparticles as antibacterials against carbapenem-resistant *Klebsiella pneumoniae* and *Acinetobacter baumannii*: a review article," *Microb. Cell Factories 2024 231*, vol. 23, no. 1, pp. 311–, Nov. 2024, doi: 10.1186/s12934-024-02584-x.
- [48] Y. Li, C. Liao, and S. C. Tjong, "Recent Advances in Zinc Oxide Nanostructures with Antimicrobial Activities," *Int. J. Mol. Sci. 2020, Vol. 21, Page 8836*, vol. 21, no. 22, p. 8836, Nov. 2020, doi: 10.3390/ijms21228836.
- [49] S. A. Sudhakar and L. S. Afinisha Deepam, "In vitro antioxidant, anti-inflammatory, antibacterial, and cytotoxic effect of *Sida cordifolia*: synthesized metal nanoparticles," *Discov. Chem. 2025 21*, vol. 2, no. 1, pp. 348–, Dec. 2025, doi: 10.1007/s44371-025-00426-2.

